
IFSCC 2025 full paper (IFSCC2025-930)

“Innovative Delivery Systems for a DNA Aptamer Promoting Hair Growth”

Paula Vela Cristobal¹, Christian Betancourt¹, Ainhoa Diaz de Pedroviejo¹, Manuel Mataix², Nuria Llera², Inés Hidalgo³, Rebeca Alonso Bartolomé¹, Francisco Jimenez⁴, Victor M. González⁵, Marta Carretero² and Sandra Freitas-Rodríguez⁶

¹ R&D, Nalon Innova SL, Oviedo; ² Center for Energy, Environment and Technology Research (CIEMAT), ³ Bioingeniería, Universidad Carlos III, Madrid, ⁴ Mediteknia Skin & Hair Lab, Gran Canaria, ⁵ Aptamer Group, IRYCIS-Hospital Ramón y Cajal, Madrid, ⁶ R&D, Nanovex Biotechnologies SL, Llanera, Spain.

1. Introduction

Hair loss is a multifactorial condition with complex biological origins and significant psychological repercussions. Beyond its clinical implications, it poses a major cosmetic concern, often affecting self-perception, confidence, and emotional well-being [1]. The increasing demand for effective, science-driven solutions has positioned hair care as a rapidly growing sector in the cosmetic and pharmaceutical industries.

In response to this challenge, our research aims to develop an innovative therapeutic strategy based on a DNA aptamer specifically designed to modulate the hair follicle cycle. By targeting key molecular pathways involved in follicular regulation, the aptamer seeks to promote follicular cell proliferation and hair shaft elongation. This approach holds potential not only for physical improvement but also for restoring self-esteem and emotional well-being in individuals experiencing hair loss. [12]

DNA aptamers are synthetic, single-stranded oligonucleotides that fold into unique 3D conformations, enabling them to bind with high specificity and affinity to various biological targets [5]. Due to their excellent biocompatibility, low immunogenicity, and chemical flexibility, they have emerged as powerful tools in modern biomedicine [2,5,11].

To ensure optimal delivery and preservation of the aptamer's structural and functional integrity, we propose a multifaceted formulation strategy comprising three complementary approaches. First, we employ lipid nanoparticles (LNPs), vesicular structures composed of ionizable lipids, helper lipids, cholesterol, and PEG-lipids. These nanoparticles form compact and

stable assemblies that facilitate cellular uptake, protect the aptamer from enzymatic degradation, and promote endosomal escape and intracellular release [2,4,6,9,10]. Second, we develop lipoplexes, which are formed through electrostatic interactions between cationic lipids and the negatively charged aptamer [2]. Finally, we explore a surface-functionalized lipid nanoparticle (fLNP) strategy, where the aptamer is covalently conjugated to the outer membrane of lipid-based carriers via bio-orthogonal chemistries—such as thiol–maleimide coupling or click chemistry—enabling improved targeting and orientation control [11].

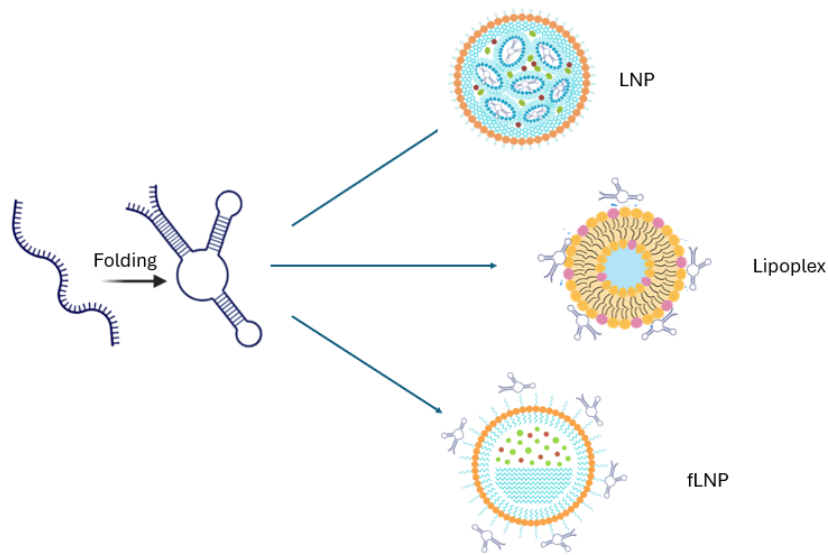


Figure 1. Schematic representation of the delivery strategies employed throughout the experimental workflow. The diagram illustrates the three approaches based on aptamer association: lipoplexes (electrostatic complexation), lipid nanoparticles (encapsulation), and surface-functionalized LNPs (chemical conjugation).

Three approaches will be systematically compared to one another and to the naked aptamer, with the goal of identifying the most suitable formulation in terms of physicochemical stability, delivery efficiency, and biological performance. Our findings underscore the potential of our platform to develop efficient delivery systems for highly specific and innovative oligonucleotide-based Cosmetic ingredients.

2. Materials and Methods

Aptamer restructuring

Prior to use, the DNA aptamer was thermally restructured to ensure proper folding. The solution was heated at 95 °C for 10 minutes to denature any preformed secondary structures, followed by immediate cooling on ice and incubation at 4 °C for an additional 10 minutes to allow proper refolding into its active conformation.

LNPs Synthesis

Lipid nanoparticles (LNPs) were synthesized using the NanoScaler microfluidic system (Knauer) for controlled particle size and encapsulation. The aqueous phase (aptamer in PBS-MgCl₂ buffer) and organic phase (lipid mix in ethanol: ionizable lipid, helper lipid, PEGylated lipid, and structural lipid at optimized molar ratios) were mixed using a crossflow micro-fluidic setup at defined flow rate ratios (FRR) and total flow rates (TFR). Ethanol was removed by overnight dialysis at 4 °C in PBS-MgCl₂.

Lipoplexes

Cationic liposomes were prepared using the thin-film hydration (TFH) method, as previously described in the literature. Briefly, the lipids used, phosphatidylcholine (PC, 23–80 mol%), cetyltrimethylammonium chloride (CTAC, 7–19 mol%), polysorbate 80 (Tw80, 1–70 mol%), and cetyl alcohol (CetylOH, 18 mol%), were weighed and dissolved in ethanol in the desired molar ratios.

The organic solvent was then removed under vacuum using a rotary evaporator (IKA RV 3), forming a uniform lipid film at room temperature in round-bottom flask. The resulting lipid film was hydrated with PBS buffer (pH 7.0) for 30 minutes and subsequently homogenized using a Polytron PT-2500 for 5 minutes.

Lipoplexes were synthesized by mixing the empty cationic liposomes with the aptamer of interest previously dissolved in nuclease-free PBS MgCl₂. The mixture was vortexed at room temperature and incubated using different liposome:aptamer ratios to allow complex formation.

Surface-functionalized lipid-based carriers

For the synthesis of membrane-functionalized LNPs, microfluidic mixing was performed using the NanoScaler system (Knauer), following the same formulation parameters as for conventional LNPs. The aqueous phase consisted solely of PBS- MgCl₂ buffer, while the organic phase contained the lipid mixture in ethanol with the standard molar ratio of ionizable lipid, helper lipid, PEGylated lipid, and structural lipid at optimized molar ratios. In this case, a defined fraction of the PEGylated lipid was replaced with a PEG-lipid conjugated to the aptamer of interest. This approach allows for aptamer display on the surface of the nanoparticles upon self-assembly, while maintaining stability.

Physicochemical Characterization

Particle size and polydispersity index (PDI) were measured by dynamic light scattering (DLS) using NanoZS90 and Zetasizer Ultra (Malvern), with particle concentration obtained from the Zetasizer Ultra. Each formulation was measured in triplicate. This study was conducted at multiple time points over a period of three months to ensure particle stability.

Encapsulation Efficiency

Encapsulation efficiency (EE) was assessed via the OligoGreen assay (Invitrogen) in the presence and absence of Triton X-100. Fluorescence was measured at 480/520 nm using a Synergy HTX reader, and EE% was calculated as:

$$\text{EE\%} = (\text{Encapsulated RNA} / \text{Total RNA}) \times 100$$

Assessment of thiol-maleimide conjugation efficiency

Aptamer-lipid conjugates were prepared by incubating thiolated aptamers with maleimide-functionalized lipids at different molar ratios at room temperature overnight. In parallel, control samples containing the same concentrations of free thiolated aptamer (without lipid) were prepared. After incubation, free thiol groups were quantified by measuring fluorescence according to the manufacturer's protocol (Measure-IT™ Thiol Assay Kit Invitrogen). The reduction in free thiol signal in the conjugated samples, compared to controls, was used to assess the efficiency of the conjugation reaction.

Quantification of aptamer complexation in lipoplexes by agarose gel electrophoresis

Agarose gel electrophoresis was used to assess the complexation of the aptamer within the lipoplexes. Samples loaded onto the gel included: (i) lipoplexes, (ii) lipoplexes treated with a chaotropic agent to disrupt electrostatic interactions without disrupting the nanoparticle structure, and (iii) free (uncomplexed) aptamer as control.

Gels were prepared with 1.5% (w/v) agarose dissolved in TBE buffer and stained with ethidium bromide (EtBr) at a final concentration of approximately 1:1000 (4 µL of EtBr per 40 mL of TBE buffer). Samples were mixed with loading buffer and loaded into the wells. Electrophoresis was performed at 85V 15 minutes and bands were visualized under UV illumination.

Cell Culture and Transfection Protocol

The following experimental procedures are currently underway and, therefore, no results are presented in the corresponding sections. However, they have been included as they will form part of the final communication to be presented at the congress.

Human keratinocytes were cultured as adherent cells in high-glucose Dulbecco's Modified Eagle Medium (DMEM) supplemented with 10% fetal bovine serum (FBS) and 1% penicillin-streptomycin. Cells were maintained at 37 °C in a humidified incubator with 5% CO₂ and passed at approximately 80% confluence using 0.05% trypsin-EDTA.

For transfection, keratinocytes were seeded one day prior to treatment to reach ~70% confluence. Cells were then incubated with LNP formulations diluted in serum- and antibiotic-free DMEM in a reduced volume for 4–6 hours. After incubation, the medium was replaced with complete growth medium, and cells were maintained at 37 °C in 5% CO₂ until further analysis.

Biological Activity Assessment

To assess the biological activity of the aptamer, the activation of the cyclic adenosine monophosphate (cAMP) signaling pathway—a known downstream effect of aptamer binding—was evaluated. A commercial cAMP detection kit (cAMP-Glo™ Max Assay) was used following the manufacturer's instructions.

3. Results

3.1 Generation of Aptamer-Compatible Nanoparticle Systems with Suitable Physicochemical Stability for Cosmetic Use

This study evaluates three delivery strategies—lipid nanoparticles (LNPs), lipoplexes, and functionalized lipid nanoparticles (fLNPs)—for a DNA aptamer designed to stimulate hair growth. The formulations were analyzed in terms of their physicochemical characteristics and preliminary biological effects, with the naked aptamer included as a control.

Table 1. Mean of particle size and polydispersity index (PDI) of the different delivery strategies.

Delivery Strategy	Size (nm)	PDI
Loaded LNPs	106 ± 8.34	0.12 ± 0.03
Lipoplexes	144 ± 16.3	0.25 ± 0.12
Functionalized LNPs	156.6 ± 6.1	0.18 ± 0.2

Values correspond to the intermediate aptamer-to-lipid molar ratio (1:1) among the tested conditions (low, medium, and high). Data are expressed as mean ± standard error of the mean (SEM) from independent measurements. PDI: polydispersity index.

As shown in **Table 1**, each formulation presented distinct size and polydispersity profiles. Loaded LNPs exhibited the smallest particle size (106 ± 8.34 nm) and the lowest PDI (0.12 ± 0.03), indicating a highly uniform population. Lipoplexes were significantly larger (144 ± 16.3

nm) and more polydisperse (PDI 0.25 ± 0.12), consistent with their electrostatic self-assembly mechanism. Functionalized LNPs (fLNPs) were the largest (156.6 ± 6.1 nm), likely due to surface conjugation of the aptamer, with a moderate PDI (0.18 ± 0.2) suggesting acceptable homogeneity.

These findings are further illustrated in **Figure 2**, which shows the particle size distribution across various aptamer-to-lipid (Apt:Lip) ratios. A dose-dependent increase in particle size was observed with increasing aptamer content, particularly in lipoplexes and fLNPs. This trend supports the hypothesis that the aptamer contributes significantly to the structural properties of the formulations and highlights the importance of ratio optimization.

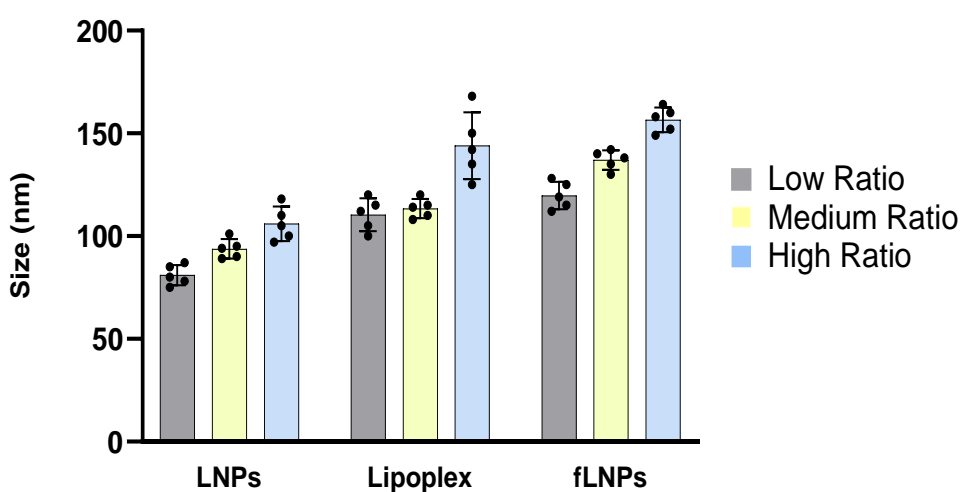


Figure 2. Size distribution of the different delivery strategies at varying aptamer-to-lipid (Apt:Lip) molar ratios. Data represent the mean particle size, with error bars indicating variability among replicates. The ratios shown in the legend correspond to the different Apt:Lip molar ratios used in each formulation.

3.2 Efficient Aptamer Complexation and Encapsulation as a Basis for Prototype Selection

Agarose gel electrophoresis was used to assess the interaction of the aptamer with the different carriers (**Figure 3**). In panel A, increasing the cationic lipid-to-aptamer ratio in lipoplexes (lanes 2–4) led to a progressive decrease in free aptamer signal, indicating more efficient complex formation. The addition of a chaotropic agent (lanes 5–7) released the aptamer, confirming that the interaction is predominantly electrostatic.

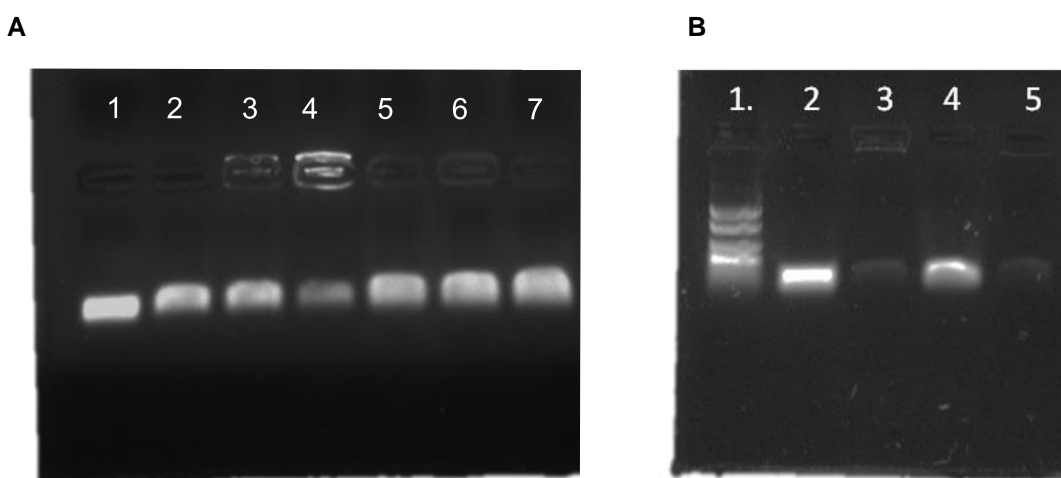


Figure 3. A. Agarose gel electrophoresis of lipoplexes formed at different cationic lipid-to-aptamer molar ratios. Lanes correspond to: (1) free aptamer; (2) lipoplex at 32:1; (3) at 720:1; (4) at 2000:1; (5–7) the same lipoplexes treated with a chaotropic agent to disrupt electrostatic interactions, respectively. A progressive increase in aptamer retention is observed with higher cationic lipid content. **B.** Agarose gel electrophoresis of lipid nanoparticles (LNPs) to evaluate aptamer encapsulation. Lanes correspond to: (2) free aptamer (control); (3) intact LNPs; (4) LNPs treated with detergent to disrupt the nanoparticle structure and release the cargo; and (5) LNPs treated with a chaotropic agent, which does not compromise nanoparticle integrity or release the encapsulated aptamer, as shown.

In panel B, intact LNPs (lane 3) showed no free aptamer band, suggesting successful encapsulation. Treatment with detergent (lane 4) disrupted the nanoparticle and released the aptamer, while chaotropic treatment (lane 5) did not, indicating that the aptamer is physically protected within the lipid matrix rather than merely surface bound.

While the biological assays are currently ongoing and results are not yet available, the aptamer evaluated in this study has been specifically designed to interact with surface receptors present in the hair follicle microenvironment. Based on prior internal studies, this interaction is hypothesized to trigger signaling cascades involved in tissue regeneration and follicular activation. Although the specific molecular target remains confidential, the design rationale is supported by early, unpublished evidence suggesting its potential role in promoting hair shaft elongation and overall follicular activity. The evaluation of its biological effects across the different delivery strategies will be included in the final communication of this work.

4. Discussion

The stimulation of follicular regeneration and hair growth remains a significant challenge in dermatology and cosmetic science. Conventional treatments often suffer from limitations related to stability, efficacy, or lack of targeted delivery, underscoring the need for innovative

strategies [1,12]. In this context, the use of delivery systems tailored to highly specific oligonucleotide-based active ingredients offer a promising alternative [2,5,11]. By combining the high selectivity and therapeutic potential of aptamers with advanced lipid-based carriers, our approach represents a novel and attractive strategy for applications in cosmetic science, particularly in hair stimulation therapies.

Among the three delivery systems evaluated—lipoplexes, lipid nanoparticles (LNPs), and surface-functionalized lipid nanoparticles (fLNPs)—all showed acceptable physicochemical stability in terms of particle size and polydispersity index (PDI). However, standard LNPs were the most robust and reproducible formulation, with consistent size and low PDI values (**Table 1; Figure 2**) [6,7]. Functionalized LNPs displayed slightly increased size and PDI values, likely due to the conjugation of aptamers on the particle surface, which can introduce additional heterogeneity. Lipoplexes, by contrast, exhibited the highest polydispersity, likely reflecting the less controlled nature of the electrostatic complexation process used in their formation [2].

Agarose gel electrophoresis (**Figure 3**) confirmed successful complexation of the aptamer with lipoplexes and effective encapsulation within LNPs. For lipoplexes, increasing the cationic lipid-to-aptamer ratio improved complexation efficiency, as evidenced by the reduction in free aptamer. However, higher lipid ratios also led to increases in particle size and PDI, suggesting a trade-off between complexation and stability. An intermediate ratio was identified as the optimal balance. In the case of LNPs, the aptamer was efficiently encapsulated and could be released upon nanoparticle disruption, confirming effective cargo loading. These findings validate the capability of our microfluidic platform to reproducibly generate both standard and functionalized lipid nanoparticles with favorable characteristics. The physicochemical results presented (**Table 1; Figure 2**) reinforce the potential of this system for further biological applications [6,7].

Although complete biological data are still being generated, initial *in vitro* transfection assays suggest that all nanocarrier-based strategies enhance the intracellular effect of the aptamer compared to its free form [5,6]. These results support the hypothesis that encapsulation improves cellular uptake and stability, mitigating common limitations associated with unmodified oligonucleotides [2,4,5]. Ongoing studies will provide further insights, and full biological results will be presented at the upcoming communication scheduled for September.

Looking ahead, current efforts are focused on expanding the biological evaluation of these systems, particularly their capacity to modulate follicular pathways involved in hair growth. These experiments are expected to shed light on the functional mechanisms of action and guide the optimization of the most promising delivery strategies. Further research will be

needed to confirm their performance in more complex models and to assess long-term efficacy and stability.

5. Conclusions

1. We successfully synthesized and characterized three distinct aptamer delivery systems—lipoplexes, LNPs, and functionalized LNPs—using a reproducible microfluidic-based formulation approach.
2. All tested delivery systems exhibited good physicochemical stability, with consistent particle size and low PDI values, supporting their potential for further development.
3. Functionalized LNPs demonstrated appropriate characteristics for biomedical applications, although their increased size and heterogeneity reflect the influence of surface modification.
4. Preliminary results validate the promise of lipid-based platforms for aptamer delivery, particularly in the context of cosmetic applications targeting follicular regeneration.

6. References

1. Zucchelli, F., Mathews, A., Sharratt, N., Montgomery, K., & Chambers, J. (2024). The psychosocial impact of alopecia in men: A mixed-methods survey study. *Skin Health and Disease*, 4(5), e420. <https://doi.org/10.1002/ski2.420>
2. Bost, J. P., Barriga, H., Holme, M. N., Gallud, A., Maugeri, M., Gupta, D., Lehto, T., Valadi, H., Esbjörner, E. K., Stevens, M. M., & El-Andaloussi, S. (2021). Delivery of oligonucleotide therapeutics: Chemical modifications, lipid nanoparticles, and extracellular vesicles. *ACS Nano*, 15(9), 13993–14021. <https://doi.org/10.1021/acsnano.1c05099>
3. Mehraji, S., & DeVoe, D. L. (2024). Microfluidic synthesis of lipid-based nanoparticles for drug delivery: Recent advances and opportunities. *Lab on a Chip*, 24(1), 123–145. <https://doi.org/10.1039/D3LC00821E>
4. Smith, S. A., Selby, L. I., Johnston, A. P. R., & Such, G. K. (2019). The endosomal escape of nanoparticles: Toward more efficient cellular delivery. *Bioconjugate Chemistry*, 30(2), 263–272. <https://doi.org/10.1021/acs.bioconjchem.8b00732>
5. Zhou, J., & Rossi, J. (2017). Aptamers as targeted therapeutics: current potential and challenges. *Nature Reviews Drug Discovery*, 16(3), 181–202. <https://doi.org/10.1038/nrd.2016.199>
6. Hou, X., Zaks, T., Langer, R., & Dong, Y. (2021). Lipid nanoparticles for mRNA delivery. *Nature Reviews Materials*, 6(12), 1078–1094. <https://doi.org/10.1038/s41578-021-00358-0>
7. Sanghani, A., Kafetzis, K. N., Sato, Y., Elboraei, S., Fajardo-Sanchez, J., Harashima, H., Tagalakis, A. D., & Yu-Wai-Man, C. (2021). Novel PEGylated lipid nanoparticles have a

- high encapsulation efficiency and effectively deliver MRTF-B siRNA in conjunctival fibroblasts. *Pharmaceutics*, 13(3), 382. <https://doi.org/10.3390/pharmaceutics13030382>
8. Huang, L., Jiang, S., & Shi, J. (2022). Microfluidic fabrication of lipid nanoparticles for drug delivery applications. *Acta Pharmaceutica Sinica B*, 12(7), 2969–2979. <https://doi.org/10.1016/j.apsb.2022.01.014>
9. Dowdy, S. F. (2017). Overcoming cellular barriers for RNA therapeutics. *Nature Biotechnology*, 35(3), 222–229. <https://doi.org/10.1038/nbt.3802>
10. Wang, P., Zhang, L., Zheng, W., Cong, L., Guo, Z., Xie, Y., Wang, L., & Tang, R. (2020). Thermo-sensitive lipid nanoparticles for enhancing the delivery of nucleic acid-based drugs. *Frontiers in Pharmacology*, 11, 952. <https://doi.org/10.3389/fphar.2020.00952>
11. Abdolahad, M., Janmaleki, M., & Salehi, P. (2022). Aptamer-functionalized nanoparticles for targeted drug delivery: Opportunities and challenges. *Advanced Drug Delivery Reviews*, 186, 114338. <https://doi.org/10.1016/j.addr.2022.114338>
12. Jin, S.-E., & Sung, J.-H. (2024). Delivery strategies of siRNA therapeutics for hair loss therapy. *International Journal of Molecular Sciences*, 25(14), 7612. <https://doi.org/10.3390/ijms25147612>